2018 IEEE International Conference on Robotics and Automation (ICRA)
May 21-25, 2018, Brisbane, Australia

A Soft Pneumatic Fabric-Polymer Actuator for Wearable Biomedical Devices: Proof of Concept for Lymphedema Treatment

Etsel Suarez[1], Juan J. Huaroto[1], Alberto A. Reymundo[2], Dónal Holland[3], Conor Walsh[4], *Member, IEEE* and Emir Vela[1†], *Senior Member, IEEE*

***Abstract*— Soft actuators are ideal candidates for wearable biomedical devices, their inherent compliance, robustness, lightweight and the possibility to be washable take advantage over rigid actuators. Thus, a soft pneumatic fabric-polymer bending actuator as a base component for a robotic device for lymphedema treatment is reported in this work. The actuator is composed of two mechanical elements, one made of fabric and the other one made of a hyperelastic polymer which is stuck on the fabric element. The fabric element is designed and fabricated with a curved shape longer than the polymer element, that is a hyperelastic beam. To assemble both elements, the fabric element was folded before sticking in order to match the length of the polymer beam. Once the air is pumped into the fabric, it bends towards its original curved shape. Once the air is removed, the hyperelastic beam allows the actuator to recover its initial position. This actuator is capable of exerting compression and lateral force on a human arm mimicking manual lymphatic drainage. A mathematical model is presented which is in good agreement with the experimental data, it could serve to predict the actuator motion. An end-tip free bending displacement of about 2.2 cm and a bending force of about 0.35 N were achieved at 12.5 kPa. A proof-of-concept system for lymphedema treatment is presented as well.**

I. INTRODUCTION

The growing field of soft robotics technology is a good candidate towards the development of medical devices/instruments [1] for physical therapy, rehabilitation, human capacity augmentation, assistive and prosthetic devices [2],[3]. In contrast to robotic systems based on rigid materials [4],[5],[6],[7], soft-robotics materials [8],[9],[10],[11] present properties that have many advantages for medical applications including but not limited to, lightweight, safe for human-robot interaction, adaptability to surroundings, washable, and so on.

This work was partially supported by the Department of Biomedical Engineering at Universidad Peruana Cayetano Heredia and the Harvard-UTEC Faculty Grant. †Corresponding author

[1]Etsel Suarez, Juan J. Huaroto and †Emir Vela are with the Department of Biomedical Engineering, Escuela Profesional de Ingenieria, Facultad de Ciencias y Filosofia, and Laboratorios de Investigacion y Desarrollo - LID, Universidad Peruana Cayetano Heredia, Lima, Peru. Emir Vela is also with the Department of Electrical and Computer Engineering, University of New Mexico - UNM, USA. etsel.suarez@upch.pe; juan.huaroto@upch.pe; emir.vela@upch.pe

[2]Alberto A. Reymundo is with the Department of Mechanical Engineering, Universidad de Ingenieria y Tecnologia - UTEC, Barranco, Lima, Peru, areymundo@utec.edu.pe

[3]Dónal Holland is with the University College Dublin, Ireland, donal.holland@ucd.ie

[4]Conor Walsh is with the School of Engineering and Applied Sciences and Wyss Institute, Harvard University, Cambridge, MA 02138 USA, walsh@seas.harvard.edu

In the case of rehabilitation therapies, the process, in general, is personalized for each patient increasing the demand for specialized physicians; as a consequence treatments become more expensive and non-ubiquitous. At present, the robotics community is making great efforts to provide novel robotic devices for rehabilitation therapies specially in the field of soft robotics [12],[3],[13],[14],[15]. In these soft devices, key components are soft actuators that can be actuated with electrical charges, chemical reactions and pressurized fluid principles.

Soft pneumatic actuators are getting more attention for wearable robotic devices due to their ease of fabrication, lightweight, safety, compliance, and low-cost. For instance, pneumatic artificial muscles (PAM) and its variants including McKibben muscles [16], pleated PAMs [17], pouch motors [18], and inverse PAMs [19].

Lymphedema is the most common disease caused by cancer, one out of five women surviving breast cancer will develop arm lymphedema [20],[21],[22]. This disease is defined as the tissue fluid accumulation that arises as a consequence of impaired lymphatic drainage. As edema progresses, it can lead to pain, infection, function decrease, reduced quality of life, body image issues and anxiety [23],[24]. There are different grades of lymphedema which depends on the volume of accumulated lymph and qualitative skin properties. The most relevant grade, where the lymphedema could be reversibly treated, is the first grade, mostly ignored. The rehabilitation therapy known as lymphedema treatment [25],[26] consist of reducing the limb volume using manual lymphatic drainage (MLD), special garments, exercises and skin care, redirecting the lymph flow to another body region to maintain the lymphatic circulation.

There exists some automatic devices to treat lymphedema [27],[28], they are based on a series of fabric pouches, pneumatically actuated, that exert compression in a sequential manner on the limb in order to emulate the MLD. However, Camerota and Aziz explained that these devices fail because they do not avoid that lymph flow back from proximal to distal regions during the intermittent compression cycles [29].

In this work, a soft pneumatic fabric-polymer-based actuator (SPFPA) for lymphatic drainage is presented to treat arm lymphedema at the first grade. This actuator performs simultaneously two movements exerting compression and lateral traction force on the skin surface, in order to address the lymph towards a drainage node. Thus, proximal lymphatic regions can be evacuated before distal ones. As the actuator

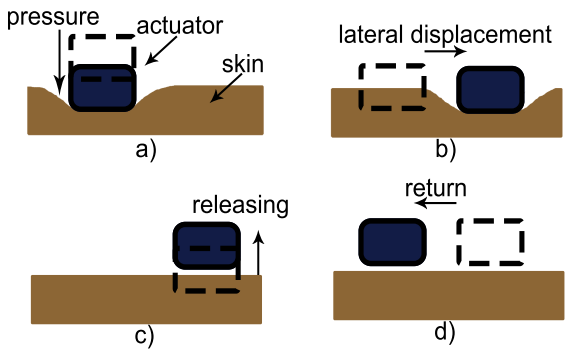

Fig. 1. Schematic showing the actuator working for Manual Lymphatic Drainage. a) Compression over the skin when FE is actuated, actuator initial position b) Lateral bending displacement and force c) Release compression and lateral force over the skin d) Actuator recovers back to its initial position when air is removed

works in contact with the skin, it is composed of a fabric-based element (FE) (part in contact with the skin), and a soft hyperelastic compliant element (SCE). So the FE compresses and exerts a lateral force on the skin when air is pumped into it. Once the air gets out the FE, the SCE ensures that the actuator returns to its initial position (see Fig. 1).

The proposed SPFPA could pave the way to new kinds of fabric-based actuators for medical applications with a very simple design, fabrication process and actuation mode. Section II deals with the actuator design emphasizing the actuator's components and its ease of fabrication. In section III, a mathematical modeling is introduced in order to predict the dynamic behavior. In section IV, the experimental results and characterization are discussed. Then, conclusions and future directions are presented.

II. ACTUATOR DESIGN

In lymphedema of first grade, a compression of 30 mmHg (4 kPa) and a lateral traction movement of the skin have to be performed [30]; and according to physicians specialized in lymphedema treatments the lateral displacement of the skin has to be of about 3 mm as a maximum. So, the SPFPA has to perform two kinds of movement on the patient's skin, a perpendicular one to compress the skin and a lateral one to force the lymph to flow towards its right direction. To this end, the SPFPA has two soft mechanical elements: a pre-shaped fabric element and a hyperelastic polymer element. The FE is designed and fabricated with a pre-shape (see Fig. 2) in order to reach a certain bending amplitude while actuation is performed; as the FE does not have elastic properties to store elastic energy, a SCE is stuck onto the FE to accomplish this task. The FE is pneumatically pressurized thus exerting a compression force on the skin (perpendicular motion), and due to its pre-shape a bending is also produced while inflating (lateral motion). The SCE, stuck on the FE, acts as a spring to recover the SPFPA initial position after removing the air inside the FE (see. Fig. 3).

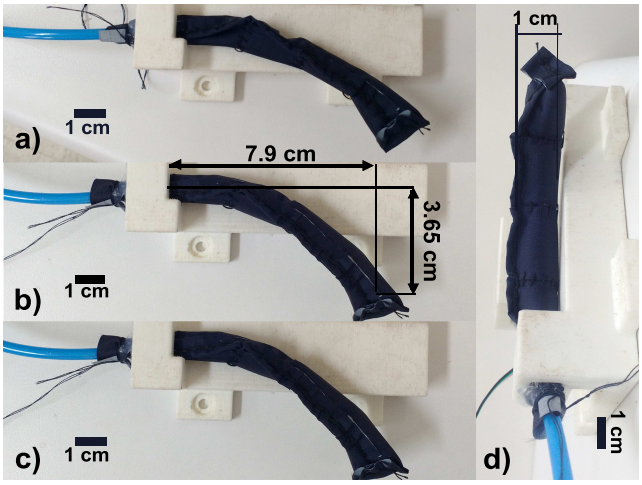

Fig. 2. a) Fabric element in its original curved shape b) Fabric with pressurized air performing a maximum bending motion c) Fabric element remains at its original shape and initial position after air is removed d) Side view of the inflated fabric

A. Fabric Element Design

The FE is made of a Ripstop Nylon plastic sheet of 14×11 cm^2 (Fig. 2). Ripstop Nylon sheet is hermetic and non-toxic, it allowed to fabricate the FE as a pre-shaped air camera simplifying the fabrication process. The sheet was sewed with thread to create folds in order to shape the FE as shown in Fig. 2. The FE has a shape of an arc of circumference with 9 cm in length, a radius of curvature of about 5.8 cm and a FE width of about 9 mm for the position shown. These dimensions are related to an average forearm width of about 7 cm where the prototype is intended to be tested. The FE will be in direct contact with a human skin, however no tests were performed yet to observe whether force friction between FE and skin can cause any damage. As aforementioned, the pressure needed for this treatment is of about 4 kPa in compression that is very low; and additionally there will not be relative motion between the skin and FE, it means FE has to draw the skin with a static force friction to accomplish the correct treatment according to physicians. Therefore, we consider that the likely damage on the skin will be insignificant. Tests on this purpose will be perform in future.

The FE is fabricated with 5 folds in the middle in order to obtain a large end-tip bending displacement as shown in Fig. 2b.

B. Soft Compliant Element Design

The idea to include a hyperelastic compliant element was to provide the capacity of storing elastic deformation energy to recover the actuator initial position after removal of pressurized air.

The SCE is a hyperelastic beam with 7.5 cm in length and a rectangular cross-section of 6 mm in width and 4 mm in height (Fig. 3c). This cross-section was chosen following the results reported by Polygerinos *et al.* [33]. They compared three different cross-sections: rectangular,

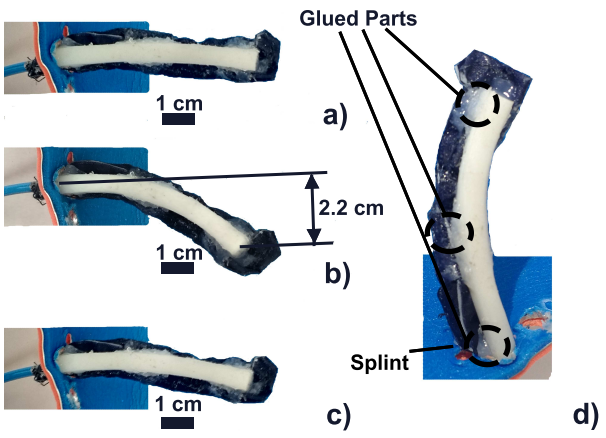

Fig. 3. a) Soft fabric-polymer actuator at its initial position fixed on a splint b) Actuator pressurized with air performing bending motion c) Return to almost the initial position under the action of the soft compliant element when air is removed. A residual deformation remains due to folds rearrangement d) The soft compliant element is glued on the fabric element in three positions with Sil-Poxy

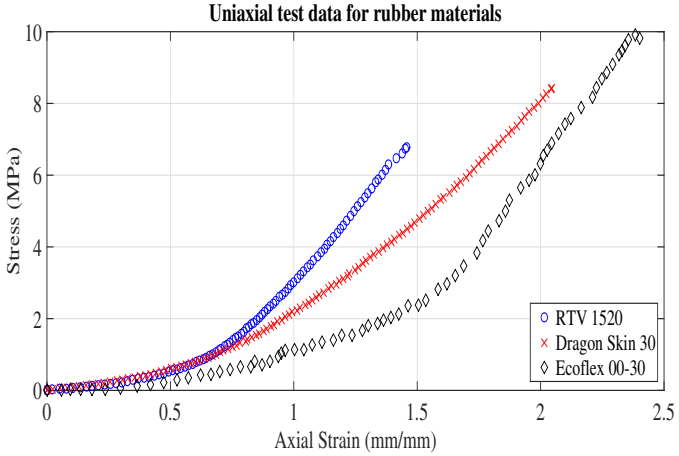

Fig. 4. Stress vs strain curve for the RTV 1520 material according to ASTM d412-06a standard test

hemi-circular and circular finding that the rectangular section has the higher bending resistance. Hence, it could store larger elastic deformation energy.

C. Fabrication

A 3D-printed mold was used to fabricate the SCE where RTV 1520 silicone rubber [34] (1:1 mixed parts) was poured. This material was preferred due to its higher stress-to-strain ratio (for axial strains between 0.7 to 1.4) according to Fig. 4. Three rectangular bases were fabricated at the bottom of the SCE to be stuck onto the FE.

To assemble both elements, the FE had to be folded to obtain the shape of the SCE, then they were stuck together using adhesive silicone Sil-Poxy from Smooth-On (cf. Fig. 3d). Thus, once the air is pumped into the FE, it will bend towards its original curved shape deforming the SCE. Once, the air is removed from the FE, the SCE will recover almost its original longitudinal shape. The FE is designed to be in contact with the skin and the SCE plays the role of the elastic component, thus by switching ON and OFF the air pump actuation cycles can be generated in a simple manner.

The SPFPA differs from recent works [31],[32] because of its ease of design and fabrication. Two materials are solely used and the FE does not need an internal additional bladder to be deformed by inflation.

III. Mathematical Modeling

A. Hyperelastic Rubber Characterization

The silicone rubber material used was RTV 1520. It was characterized following ASTM D412-06a "Standard Test Methods for Vulcanized Rubber and Thermoplastic Elastomers-Tension" [35] using a Zwick Roell Z050 testing machine at a speed of 180 mm/min and a preload of 30 gr. Data in Fig. 4 shows the higher stress-to-strain ratio of RTV 1520 in comparison with other commercially available polymers. This feature suits for the design of the proposed SCE.

To describe the material behavior, a 3 parameters Mooney-Rivlin constitutive model was used [36] according to the curve obtained in Fig. 4.

The 3 parameters (eq. 1) of Mooney Rivlin Constitutive Model was calculated using the Engineering Data Component System from ANSYS® 16.0 by introducing the data shown in Fig. 4 for RTV 1520 material.

$$\begin{aligned} C_{10} &= -1.138\ MPa, \\ C_{01} &= 1.389\ MPa, \\ C_{11} &= 0.569\ MPa. \end{aligned} \tag{1}$$

B. Actuator Dynamic Model

A dynamic model using the calculated parameters is proposed to predict the behavior of the SPFPA for further closed-loop control applications.

The parameters allowed to find the strain energy density function for an incompressible hyperelastic material, defined as

$$W = C_{10}\,(I_1-1)+C_{01}\,(I_2-1)+C_{11}\,(I_1-1)\,(I_2-1) \tag{2}$$

Where, I_1, I_2 and I_3 are principal invariants of Cauchy - Green tensor. The invariants are defined by three principal stretch ratios λ_1, λ_2 and λ_3 (axial, circumferential and radial directions), then

$$I_1 = \lambda_1^2 + \lambda_2^2 + \lambda_3^2 \tag{3}$$

$$I_2 = \lambda_1^2\,\lambda_2^2 + \lambda_2^2\,\lambda_3^2 + \lambda_3^2\,\lambda_1^2 \tag{4}$$

$$I_3 = \lambda_1^2\,\lambda_2^2\,\lambda_3^2 = 1 \tag{5}$$

To calculate the principal nominal stresses, the following equation was used, which depends on the strain energy density function and the principal stretch ratios, where p is the Lagrange multiplier.

$$s_i = \frac{\partial W}{\partial \lambda_i} - \frac{p}{\lambda_i} \tag{6}$$

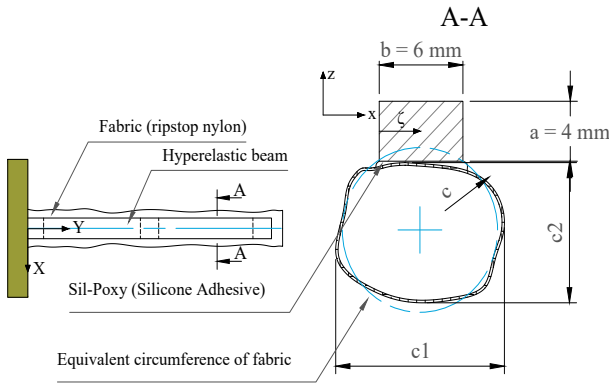

Fig. 5. Schematic and section view of the soft pneumatic fabric-polymer actuator

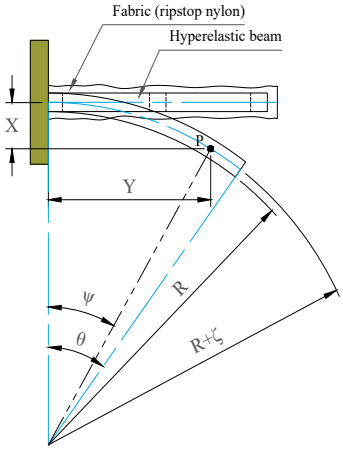

Fig. 6. Coordinates of a point belonging to the soft compliant element

To simplify the calculations, it was assumed that only axial deformation ratio exists, in this way $\lambda_2 \approx 1$ (because SCE does not rotate with respect to its axial axis), then $\lambda_1 = \lambda$ and $\lambda_3 = \frac{1}{\lambda}$ (considering eq. 5).

By replacing the values of stretch ratios and energy density in (6), the principal nominal stresses are represented as follows:

$$\begin{aligned} s_1 &= \frac{\partial W}{\partial \lambda_1} - \frac{p}{\lambda_1} \\ &= 2\,C_{10}\,(\lambda - \frac{1}{\lambda}) + 2\,C_{01}\,(1 - \frac{1}{\lambda^3}) \\ &\quad + 6\,C_{11}\,(\lambda^2 - \lambda - 1 + \frac{1}{\lambda^2} + \frac{1}{\lambda^3} - \frac{1}{\lambda^4}) \end{aligned} \tag{7}$$

$$s_2 = \frac{\partial W}{\partial \lambda_2} - \frac{p}{\lambda_2} \tag{8}$$

$$s_3 = \frac{\partial W}{\partial \lambda_3} - \frac{p}{\lambda_3} = 0 \tag{9}$$

Where s_3 is equal to zero because SCE is a solid beam not presenting stresses in radial direction. Then, the Lagrange multiplier was defined as

$$p = \frac{\partial W}{\partial \lambda_3}\,\lambda_3 \tag{10}$$

During the free bending of the actuator, the bending torque due to air pressure in the FE is in equilibrium with the moment of stresses due to the SCE bending [33], then

$$M_a = M_\theta \tag{11}$$

To determine the bending torque due to air pressure (M_a), the FE cross-section was considered as a circumferential ring with thickness $t \to 0$ [33] (cf. Fig. 5); besides the loss in torque due to air pressure leaks was considered negligible, then

$$M_a = (P_1 - P_{atm})\,\pi\,c^3 \tag{12}$$

Where c is a parameter representing the average of c_1 and c_2 in the FE cross-section and $(P_1 - P_{atm})$ is the measured manometric pressure given by a sensor.

In order to compute the moment of stresses due to the SCE bending, the following equation was used:

$$M_\theta = s_1 \int_0^b \int_0^a x\,dz\,dx \tag{13}$$

$s_1 = s$ was taken because we considered a beam model for the range of stretches, and s_2 was considered negligible. Next, for the calculation of uniaxial stretch, according to Fig 6, the following expression was obtained:

$$\lambda = \frac{R + \zeta}{R} = \frac{L/\theta + \zeta}{R} \tag{14}$$

Where ζ is the local coordinate along the SCE cross-section (for calculations $\zeta = \frac{b}{2}$ was considered).

To compute the coordinates of the positions along the SCE beam per input pressure, the following equations were used:

$$X = (R + \zeta)\,(1 - \cos(\psi)) \tag{15}$$

$$Y = (R + \zeta)\,\sin(\psi) \tag{16}$$

Where ψ represents the corresponding angle for any point of the SCE central line (Fig 6).

Finally, combining equations (11), (12), (13), (14), (15) and (16), the values of θ, the angle corresponding to the end-tip displacement, were computed as a function of the manometric pressure given by a sensor. Then, the positions of the SCE end-tip were computed.

IV. RESULTS AND DISCUSSIONS

A. Soft Actuator Characterization

The systems shown in Fig. 7 and 8 were designed to measure the lateral bending force of the SPFPA. The end-tip of the SCE was attached with a nylon thread, this latter was also attached to a CZL635 micro load cell (0-5Kg); so by pressurizing the actuator its end-tip pulls the thread and the pulling force is measured by the load cell for different input pressures. The pressure inside the actuator was controlled with a Global Modular Pressure Regulator - P31R Series (Parker Hannifin Corporation), and it was measured with an ASDX 100PGAA5 Honeywell pressure sensor, then the

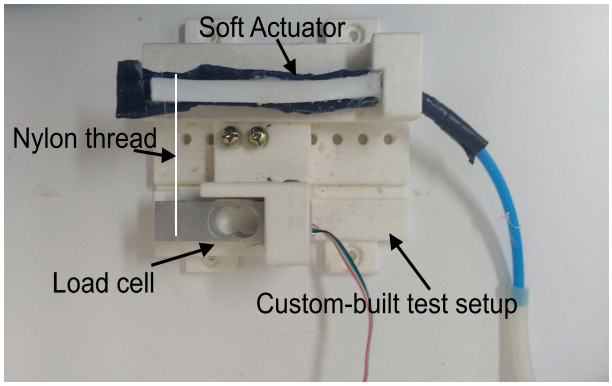

Fig. 7. Custom-built device to measure lateral bending forces

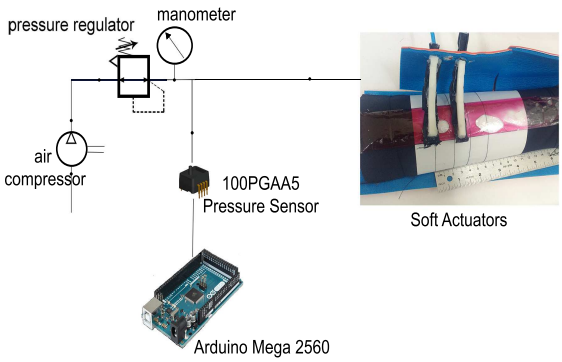

Fig. 8. Schematic of the experimental setup

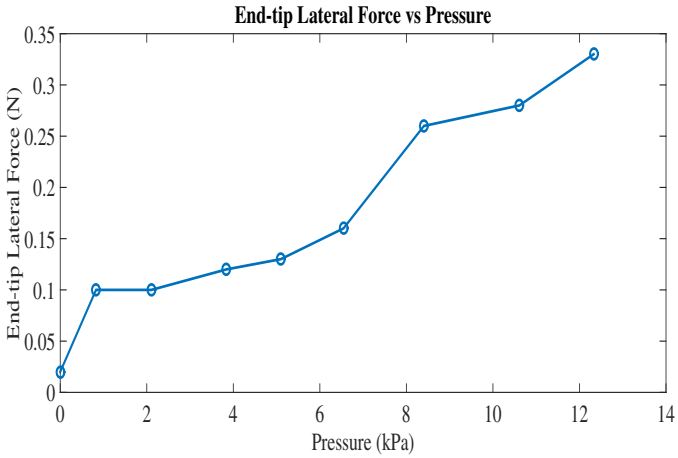

Fig. 9. Measurements of the actuator end-tip bending force as a function of input air pressure. Standard deviation of about ± 0.02 N

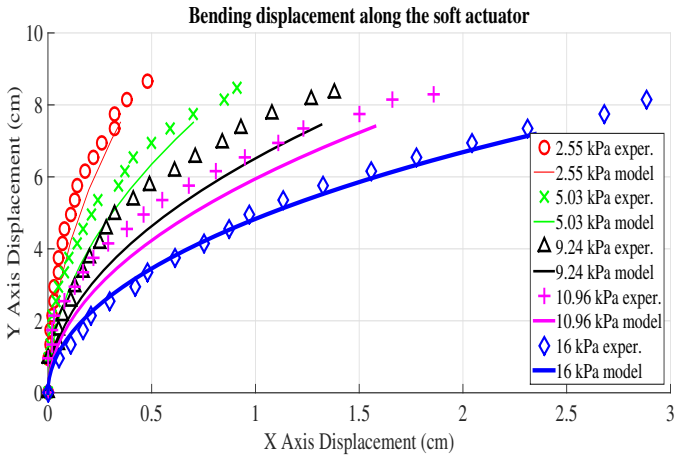

Fig. 10. Comparison between the model and experimental data for different input pressures

data was acquired and observed with an Arduino Mega 2560 board (Fig. 8).

Fig. 9 shows a non-linear behavior of the measured lateral bending force with respect to the input pressure. This could be due to the effect of the air flow entering the actuator and unfolding the FE. For 12.5 kPa of pressure a force of about 0.35 N was obtained.

Fig. 10 shows the bending positions of the SPFPA along its central line with respect to input pressures. For a 12.5 kPa of air pressure the end-tip bending was of about 2.2 cm in the X-direction or lateral direction.

B. Comparison between the Model and Experimental Data

Fig. 10 shows the experimental data obtained by measuring the positions of the SPFPA center line while bending for different input pressures; they were obtained by image processing. Besides, data obtained with the proposed mathematical bending model is presented as well to compare with the experimental data. It is observed that the model is in good agreement with the experiments; however for all pressures evaluated the experimental data is a little higher than the model data in the X and Y-direction, it could be because the FE is folded before being stuck with the SCE and while inflating FE unfolds and stretches the SCE. In addition, the model only considers an unidimensional deformation but actually it deforms in three dimensions. Nevertheless, the proposed model fitted quite good the experiments and could be used to predict the actuator end-tip position.

V. Proof of Concept for Lymphedema Treatment

The SPFPA was designed to mimic a MLD on human arms. This treatment is performed by compressing the skin and then drawing it very gently in a direction towards the body trunk. The SPFPA has a longitudinal shape of 8 cm in length and 0.9 cm in width. So it can work on a forearm. In [28] a compression pressure of 4 kPa was reported. According to the experimental data shown in Fig. 10, the SPFPA is capable of delivering this compression pressure. In addition, with the actuator bending, lymph can be pushed towards the body trunk. Although no data was found in the literature related to the friction or traction force along the surface of the skin needed for MLD, the measured forces are enough for the treatment. It means, by taking into account the maximum lateral displacement of the skin, for this kind of treatment, of about 3 mm, a preliminary test was performed on an individual's arm by pulling the skin with

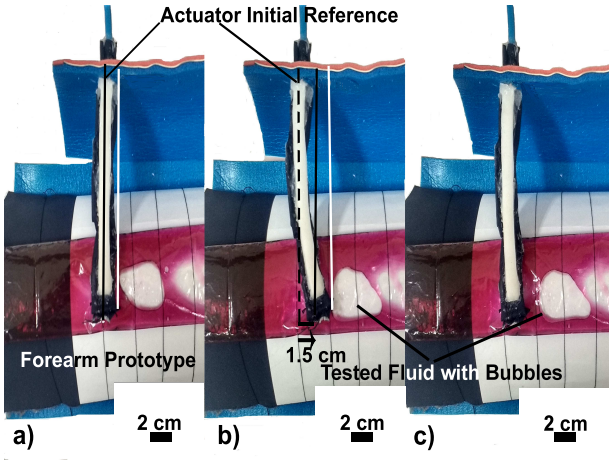

Fig. 11. (Multimedia view) A proof of concept of a system based on soft fabric-polymer actuators for mimicking MLD a) Initial position of the actuator and air bubble b) Actuator pushing forward the bubble c) The actuator recovered its initial position after air pressure was removed

different loads, finding 0.29 N for a displacement of about 3 mm. Fig. 11 illustrates a proof-of-concept experiment for lymphedema treatment. A SPFPA is fixed on a malleable splint, then it is pneumatically actuated in order to compress and laterally push on a flexible polyethylene tube filled with colored water. An air bubble was introduced inside the tube in such a manner that the actuator pushes it while compressing the tube. 1.5 cm bubble displacement was measured by activating one actuator at 12.5 kPa of pressure. The loss of about 0.7 cm in displacement is due to the interaction forces between the FE and plastic tube. This interaction is not yet studied in order to optimize the actuator design.

The idea is to have several SPFPAs in series, according to the patient's need, that can be actuated in a sequential manner and at a certain frequency.

VI. Conclusions and Perspectives

A soft pneumatic fabric-polymer-based actuator is proposed for wearable biomedical robotic devices. The actuator consists of two soft mechanical components, one made of fabric and the other one of hyperelastic polymer. Both components are fabricated separately and stuck together with a silicone glue. The main contribution of this work is the creation of an actuator capable of bending by inflating a pre-shaped fabric-based element and recovering its original shape after actuation through a polymer-based hyperelastic element. To this, the FE was designed and fabricated with a curved shape then it was folded to match the longitudinal shape of the SCE. In other words, when air is pumped into the FE, it starts unfolding to find its original curved-shape (bending); once the air is removed, the FE folds back by the action of the SCE thus SPFPA recovers its initial position. Cycles of bending can be performed by only switching ON and OFF the air pump.

The actuator achieved a free bending of about 2.2 cm and a force of 0.35 N at 12.5 kPa. A bending motion of 1.5 cm was reached in the proof-of-concept system for the same input pressure. The interaction between the actuator and the water-filled plastic tube reduced the displacement of about 32%. However, it was actuated with a low pressure, so by optimizing the actuator and increasing the pressure we expect to obtain a greater lateral displacement of the skin.

We consider to study the interactions between human skin and fabric-based elements according to [37],[38] in order to optimize the proposed design. This is important as the actuator is intended to be a medical device for lymphedema treatment, it means to work in contact with the skin. By arranging several actuators in series on a splint, a wearable robotic device can be built in order to deliver personalized treatments in hospitals or at home.

SPFPA could pave the way for new personalized low cost and easy-fabricated wearable devices where a soft compliant element could be designed in order to mechanically program a pneumatically actuated fabric-based element.

Acknowledgment

We thank Rocío Lavado and Andrea Valladares from la Escuela Profesional de Tecnología Médica, Universidad Peruana Cayetano Heredia - UPCH, for the fruitful discussions about lymphedema treatment and MLD.

References

[1] A. De Greef, P. Lambert, and A. Delchambre, "Towards flexible medical instruments: Review of flexible fluidic actuators," *Precis. Eng.*, vol. 33, no. 4, pp. 311-321, 2009.

[2] G. Belforte, G. Eula, A. Ivanov, and S. Sirolli, "Soft Pneumatic Actuators for Rehabilitation," *Actuators*, vol. 3, no. 2, pp. 84-105, 2014.

[3] P. Polygerinos, Z. Wang, K. C. Galloway, R. J. Wood, and C. J. Walsh, "Soft robotic glove for combined assistance and at-home rehabilitation," *Rob. Auton. Syst.*, vol. 73, pp. 135-143, 2015.

[4] K. C. Jones and Winncy Du, "Development of a massage robot for medical therapy," *Proc. 2003 IEEE/ASME Int. Conf. Adv. Intell. Mechatron.*, Kobe, Japan, July 2003, pp. 1096-1101 vol.2.

[5] J. Pusey, A. Fattah, S. Agrawal, E. Messina and A. Jacoff, "Design and workspace analysis of a 6-6 cable-suspended parallel robot," *Proc. 2003 IEEE/RSJ Int. Conf. Intell. Rob. Syst.*, Nevada, USA, October 2003, pp. 2090-2095 vol. 3.

[6] H. Koga, Y. Usuda, M. Matsuno, Y. Ogura, H. Ishii, J. Solis, A. Takanishi and A. Katsumata, "Development of Oral Rehabilitation Robot for Massage Therapy," *6th Int. Special Topic Conf. Info. Tech. App. Biomed.*, Tokyo, 2007, pp. 111-114.

[7] H. Lee, W. Kim, J. Han, and C. Han, "The technical trend of the exoskeleton robot system for human power assistance," *Int. J. Precis. Eng. Manuf.*, vol. 13, no. 8, pp. 1491-1497, 2012.

[8] Y. Sun, Y. S. Song and J. Paik, "Characterization of silicone rubber based soft pneumatic actuators," *2013 IEEE/RSJ Int. Conf. Intell. Robot. Syst.*, Tokyo, Japan, November 2013, pp. 4446-4453.

[9] Holland, D., Park, E., Polygerinos, P., Bennett, G., Walsh, C., "The Soft Robotic Toolkit: Shared Resources for Research and Design," Soft Robotics, Sept 2014, 1(3): 224-230.

[10] G. Agarwal, N. Besuchet, B. Audergon, and J. Paik, "Stretchable Materials for Robust Soft Actuators towards Assistive Wearable Devices," *Sci. Rep.*, vol. 6, no. 1, p. 34224, 2016.

[11] Holland, D., Abah, C., Velasco Enriquez, M., Herman, M., Bennett, G., Vela, E., Walsh, C. "The Soft Robotics Toolkit: Strategies for Overcoming Obstacles to the Wide Dissemination of Soft-Robotic Hardware," IEEE Robotics And Automation Magazine, 24.1 57-64, 2017.

[12] Y. L. Park, J. Santos, K. G. Galloway, E. C. Goldfield, and R. J. Wood, "A soft wearable robotic device for active knee motions using flat pneumatic artificial muscles," *2014 IEEE Int. Conf. Rob. Autom.*, Hong Kong, 2014, pp. 4805-4810.

[13] H.K. Yap, J.H. Lim, F. Nasrahllah, J.C.H. Goh, C.H. Yeow. "A Soft Exoskeleton for Hand Assistive and Rehabilitation Application using Pneumatic Actuators with Variable Stiffness", *in IEEE Int. Conf. Robotics and Automation (ICRA 2015)*.

[14] A. A. Reymundo, E. M. Munoz, M. Navarro, E. Vela, and H. I. Krebs, "Hand Rehabilitation using Soft-Robotics *," *2016 6th IEEE Int. Conf. Biomed. Rob. Biomechatron.*, Singapore, June 2016, pp. 698-703.

[15] A. Borboni, M. Mor, and R. Faglia, "Gloreha - Hand Robotic Rehabilitation: Design, Mechanical Model, and Experiments," *J. Dyn. Syst. Meas. Control*, vol. 138, no. 11, p. 111003, 2016.

[16] G. K. Klute, J. M. Czerniecki, and B. Hannaford, "McKibben artificial muscles: pneumatic actuators with biomechanical intelligence,"*1999 IEEE/ASME Int. Conf. Adv. Intell. Mechatron.*, Atlanta, GA, USA, 1999, pp. 221-226.

[17] F. Daerden, "Conception and Realization of Pleated Pneumatic Artificial Muscles and their Use as Compliant Actuation Elements," Ph.D. dissertation, Dept. Mech. Eng., Vrije Universitei Brussel, Belgium, 1999.

[18] R. Niiyama, X. Sun, C. Sung, B. An, D. Rus, and S. Kim, "Pouch Motors: Printable Soft Actuators Integrated with Computational Design," *Soft Rob.*, vol. 2, no. 2, pp. 59-70, 2015.

[19] E. W. Hawkes, D. L. Christensen, and A. M. Okamura, "Design and implementation of a 300% strain soft artificial muscle," in *Proc. IEEE Int. Conf. Robot. Autom.*, Stockholm, Sweden, May 2016, no. 1, pp. 4022-4029.

[20] B. Smoot, J. Wong, B. Cooper, L. Wanek, K. Topp, N. Byl, and M. Dodd, "Upper extremity impairments in women with or without lymphedema following breast cancer treatment," *J. Cancer Surviv.*, vol. 4, no. 2, pp. 167-178, 2010.

[21] F. Kouakou, V. Loue, A. Kouame, R. Adjoby, S. Koui, H. Koim, and E. Gbary, "Endometrial osseous metaplasia and infertility: A case report," *Clin. Exp. Obstet. Gynecol.*, vol. 39, no. 4, pp. 559-561, 2012.

[22] T. DiSipio, S. Rye, B. Newman, and S. Hayes, "Incidence of unilateral arm lymphoedema after breast cancer: A systematic review and meta-analysis," *Lancet Oncol.*, vol. 14, no. 6, pp. 500-515, 2013.

[23] K. L. Campbell, A. L. Pusic, D. S. Zucker, M. L. McNeely, J. M. Binkley, A. L. Cheville, and K. J. Harwood, "A prospective model of care for breast cancer rehabilitation: Function," *Cancer*, vol. 118, no. SUPPL.8, pp. 2300-2311, 2012.

[24] E. D. Paskett, J. A. Dean, J. M. Oliveri, and J. P. Harrop, "Cancer-related lymphedema risk factors, diagnosis, treatment, and impact: A review," *J. Clin. Oncol.*, vol. 30, no. 30, pp. 3726-3733, 2012.

[25] Interantional Society of Lymphology ISL, "The diagnosis and treatment of peripheral lymphedema: 2013 consensus document of the international society of lymphology,"*Lymphology*, vol. 46, no. 1, pp. 1-11, 2013.

[26] M. Bozkurt, L. J. Palmer, and Y. Guo, "Effectiveness of Decongestive Lymphatic Therapy in Patients with Lymphedema Resulting from Breast Cancer Treatment Regardless of Previous Lymphedema Treatment," *Breast J.*, vol. 23, no. 2, pp. 154-158, 2017.

[27] N. Lee, J. Wigg, S. Pugh, J. Barclay, and H. Moore, "Lymphoedema management with the LymphFlow Advance pneumatic compression pump.," *Br. J. Community Nurs.*, vol. 21, no. Suppl 10, pp. S13-S19, 2016.

[28] S. Mestre, C. Calais, G. Gaillard, M. Nou, M. Pasqualini, B. Amor C an I. Quere, "Interest of an Auto-Adjustable Nighttime Compression Sleeve (MOBIDERM Autofit) in Maintenance phase of upper limb lymphedema: the MARILYN pilot RCT", *J. Support Care Cancer*, vol. 25, no. 8, pp. 2455-2462, 2017.

[29] A. Comerota and F. Aziz, "The case for intermittent pneumatic compression," *J. Lymphoedema*, vol. 4, no. 2, pp.57-64, 2009.

[30] J.A. Petrek, P.I. Pressman, and R.A. Smith, "Lymphedema: current issues in research and management," *Cancer J. Clin.*, vol. 50, no. 5, pp. 211?292, 2000.

[31] H.K. Yap, P.M. Khin, T.H. Koh, Y. Sun, X. Liang, J. H. Lim and C.H. Yeow , "A Fully Fabric-Based Bidirectional Soft Robotic Glove for Assistance and Rehabilitation of Hand Impaired Patients," *IEEE Robot. Autom. Lett.*, vol. 2, no. 3, pp.1383-1390, 2017.

[32] H.K. Yap, F. Sebastian, C. Wiedeman and C.H. Yeow , "Design and Characterization of Low-Cost Fabric-Based Flat Pneumatic Actuators for Soft Assistive Glove Application," *Int. Conf. Rehab. Rob. ICORR*, pp.1465-1470, 2017.

[33] P. Polygerinos, Z. Wang, J. T. B. Overvelde, K. C. Galloway, R. J. Wood, K. Bertoldi, and C. J. Walsh, "Modeling of Soft Fiber-Reinforced Bending Actuators," *IEEE Trans. Robot.*, vol. 31, no. 3, pp. 778-789, 2015.

[34] Available at http://silikamoldeseinsumos.com/

[35] ASTM International. *Standard Test Methods for Vulcanized Rubber and Thermoplastic Elastomers-Tension*. Available at http://www.astm.org/cgi-bin/resolver.cgi?D412-15a.

[36] N. Kumar and V. Venkateswara Rao, "Hyperelastic Mooney-Rivlin Model: Determination and Physical Interpretation of Material Constants," *MIT Int. J. Mech. Eng.*, vol. 6, no. 1, pp. 43-46, 2016.

[37] S. Derler and L. C. Gerhardt, "Tribology of skin: Review and analysis of experimental results for the friction coefficient of human skin," *Tribol. Lett.*, vol. 45, no. 1, pp. 1-27, 2012.

[38] S. Derler, U. Schrade, and L. C. Gerhardt, "Tribology of human skin and mechanical skin equivalents in contact with textiles," *Wear*, vol. 263, no. 7, p. 1112-1116, 2007.